Compression of femtosecond petawatt laser pulses in a plasma under the conditions of wake-wave excitation

A. A. Balakin, A. G. Litvak, V. A. Mironov, and S. A. Skobelev*
Institute of Applied Physics, Nizhny Novgorod, Russia
(Received 26 December 2012; published 20 August 2013)

We propose the concept of a plasma compressor capable of producing extremely short relativistic laser pulse, which is based on the studies of self-focusing of high-power laser pulses under the wake-wave excitation conditions. It is shown that, in the optimal regime, the compression of laser pulses up to a duration of one optical cycle is possible. We study the influence of hose instability on the process of pulse self-compression and have found that this instability is not important for a wide set of initial conditions. The matter is that the length of pulse distortion in both transverse and longitudinal directions is larger than the length of the pulse self-compression. Hose instability gives only negligible decrease of compression degree and weak deformation of pulse profile.

DOI: 10.1103/PhysRevA.88.023836 PACS number(s): 42.65.Jx, 42.50.−p

I. INTRODUCTION

Development of methods for generation of optical pulses being a few optical cycles long is one of the most important research directions in the field of coherent and nonlinear optics. Optical pulses with durations shorter than 10 fs are required in a wide range of both basic and applied research, specifically, from spectroscopy with high time resolution, which allows one to study high-speed processes [1], to laser methods of particle acceleration [2]. The possibility of using extremely short pulses for generation of terahertz video pulses [3] and attosecond pulses [4,5] in the vacuum-UV and soft-x-ray ranges is actively discussed.

A decrease in the duration, i.e., compression of ultrashort laser pulses, is achieved by using special methods. Two main stages can be discerned in the compression process, namely, spectrum widening and pulse compression proper. Modern compression methods use spectrum widening at the first stage. Different nonlinear mechanisms of spectrum widening are used to solve this problem. In order to increase the spectral width of a pulse, the pulse is transmitted through a nonlinear medium whose refractive index changes on exposure to the electric field of a light wave. Specifically, for high-power laser pulses, it was proposed to use a hollow dielectric capillary filled with a gaseous medium under the conditions of predominant Kerr [6] or ionization [7,8] nonlinearity. Note that the use of the capillary in this case is aimed at solving the key problem of the interaction between laser pulses with media, namely, the increase in the interaction length, since the length of the efficient nonlinear interaction in free space is limited by diffraction divergence of the laser beam. A set of prisms or diffraction gratings is generally used for the compression proper. Another efficient way to generate extremely short pulses is to use controlled-dispersion mirrors.

In recent years, various schemes of self-compression of laser pulses in wave-guiding systems, which also use the Kerr [9] and ionization [10,11] nonlinearities, have been discussed intensively. Specifically, the possibility to generate extremely short pulses at a multi-mJ energy level was demonstrated in [11].

It's the use of the filamentation process in free space that increases the spectral width of a laser pulse at a milli-joule power level. Filaments are nonlinear structures, which exist due to the balance of focusing related to the Kerr nonlinearity and diffraction and defocusing related to the ionization nonlinearity. The filament structure of the ionized region is capable of ensuring a fairly long path for the interaction of a laser pulse with media. Pulse compression is observed when a single filament is present, which is formed in a gas under a relatively high pressure at the power of the pulse, which is only slightly higher than the critical self-focusing power [12]. However, as the detailed analysis performed in [13,14] shows, the energy efficiency of this method, i.e., the share of the initial energy in the compressed part of the laser pulse at the output from the nonlinear medium, is not high and amounts to several percent.

In this paper, we will consider self-compression of laser pulses with relativistically strong amplitudes. For such pulses, the inertia of the nonlinear response is related to the excitation of a plasma wake wave. Shortening of a pulse with a length being approximately equal to the plasma wavelength was discussed in [15], where the pulse compression by several times was demonstrated. In this paper, we will consider a mechanism of pulse shortening, which is related basically to the dynamic of radiation self-focusing under the conditions of excitation of the plasma wake wave with the period being much larger than the duration of the laser pulse. We propose a theoretical model which shows the relation between pulse self-compression and its nonstationary self-action. This model predicts that, under optimal conditions, the pulse can be compressed significantly. Numerical simulations for such conditions show that initial pulses can be compressed by about 10 times.

The paper is structured as follows. Section II defines a system of equations which describes the evolution of wideband laser radiation under the conditions of plasma wake-wave excitation. Section III present analysis of the pulse spectrum modification. Section IV studies a promising mechanism of laser-pulse shortening. Last Sec. V presents the results of studying the stability of the self-compression regime in the case of relativistically strong pulses.

*sksa@ufp.appl.sci-nnov.ru

 ©2013 American Physical Society

II. PROBLEM FORMULATION AND INITIAL EQUATIONS

The wave equation for the vector potential $\boldsymbol{A}$ has the following form for an electromagnetic wave packet propagating along z axis:

$$\frac{\partial^2 \boldsymbol{A}}{\partial z^2} + \Delta_\perp A - \frac{1}{c^2}\frac{\partial^2 \boldsymbol{A}}{\partial t^2} = -\frac{4\pi}{c}\boldsymbol{j}_\perp, \tag{1}$$

where $\Delta_\perp = \partial^2/\partial r^2 + 1/r\partial/\partial r$ and $\boldsymbol{j}_\perp$ is the transverse current. One can use quasi-one-dimensional hydrodynamics to derive an equation for $\boldsymbol{j}_\perp(\boldsymbol{A})$ in the case of laser pulses with the typical transverse scale being much larger than the plasma wavelength c/ω_{pl} ($\omega_{pl} = \sqrt{4\pi N e^2/m}$ is the plasma frequency). For circularly polarized radiation $\boldsymbol{A} = (\boldsymbol{x_0} + i\,\boldsymbol{y_0})A$, we have

$$\frac{\partial n}{\partial t} + \frac{\partial}{\partial z}\frac{np}{\sqrt{1+p^2+a^2}} = 0, \tag{2a}$$

$$\frac{\partial p}{\partial t} = \frac{\partial}{\partial z}(\phi - \sqrt{1+p^2+a^2}), \tag{2b}$$

$$\frac{\partial^2 \phi}{\partial z^2} = \frac{\omega_{pl}^2}{\omega_0^2}(n-1). \tag{2c}$$

Here, n is the electron density normalized by the density N in the absence of an electromagnetic field; the momentum p is normalized by mc, $a = eA/mc^2$, $\phi = e\Phi/mc^2$ is the normalized scalar potential, $t = \omega_0 t_{\text{old}}$, $z = z_{\text{old}}\omega_0/c$, and ω_0 is the carrier frequency.

The one-dimensional description of the excitation dynamics of the wake field by means of Eq. (2) is justified for the wave fields with the characteristic transverse scale $L_\perp$ being much longer than the length c/ω_{pl} of the plasma wave. Moreover, we consider laser pulses with the longitudinal scale (duration) $L_{||}$ being shorter than the plasma wavelength ($L_{||} < c/\omega_{pl}$).

Let us derive the condition of absence of the bubble regime. One can estimate the transverse shift of the electron $\boldsymbol{x}_\perp$ using the equation for the electron motion $d\boldsymbol{p}_\perp/dt \sim -e^2/mc^2\nabla_\perp|A|^2$. It yields the shift $\boldsymbol{x}_\perp \simeq a^2 L_{||}^2/L_\perp$. This shift will be small in comparison with the pulse radius if $a \ll L_\perp/L_{||}$, which is the applicability condition for our approach. This condition can be easily satisfied for ultrashort laser pulses $L_{||} \ll L_\perp$. Hence the electron dynamics will take place mostly in the longitudinal direction since the time of transit through the pulse in the longitudinal direction is short as compared with one in the transverse direction. As a result, we can consider laser self-action under conditions of quasi-one-dimensional plasma-wave excitation [16] [Eqs. (13)–(23)] [i.e., neglect transverse plasma flows] in contrast with the bubble regime.

We can assume that nonlinear media response (2) depends on $\tau = t - z/c$ for rare plasma where group velocity is almost equal to the speed of light c. Using integrals of equation (2) for localized distributions of density, momentum, and field,

$$n + np/\sqrt{1+p^2+a^2} = 1, \quad p + \sqrt{1+p^2+a^2} = 1+\phi,$$

we obtain expressions for n and p:

$$n = \frac{1}{2}\left(1 + \frac{1+a^2}{(1+\phi)^2}\right), \tag{3a}$$

$$p = \frac{(1+\phi)^2 - 1 - a^2}{2(1+\phi)}. \tag{3b}$$

Finally, we obtain the expression for $\boldsymbol{j}_\perp(\boldsymbol{A})$,

$$\frac{4\pi}{c}j_\perp = 4\pi N e\frac{an}{\sqrt{1+p^2+a^2}} = \frac{\omega_{pl}^2}{c^2}\frac{A}{1+\phi}, \tag{4}$$

and an equation for scalar potential,

$$\frac{\partial^2 \phi}{\partial \tau^2} = \frac{\omega_{pl}^2}{2\omega_0^2}\left[\frac{1+a^2}{(1+\phi)^2} - 1\right]. \tag{5}$$

For further detailed analysis we will use the method of reducing the wave equation to that with a mixed derivative, which works well for ultrashort pulses. Since the plasma is transparent $\omega_{pl}^2 \ll \omega_0^2$, we reduce the wave equation to the approximate one, which neglects the wave reflection. That is, it assumes the smoothness of plasma variations on the wavelength scale and the smallness of the transverse beam scale of the field over the longitudinal one (paraxial case). This approach was used to study the propagation of wave fields having the spectrum width approximately equal to the central frequency in the linear and nonlinear media [11,17,18].

As a result, we obtain the following system of dimensionless equations for the axisymmetric ultrashort circularly polarized laser-pulse dynamics in the process of nonstationary excitation of the wake wave:

$$\frac{\partial^2 a}{\partial \tilde{z}\partial\tau} + \frac{\beta a}{1+\phi} = \frac{\partial^2 a}{\partial \tilde{r}^2} + \frac{1}{\tilde{r}}\frac{\partial a}{\partial \tilde{r}}, \tag{6a}$$

$$\frac{\partial^2 \phi}{\partial \tau^2} = \frac{\omega_{pl}^2}{2\omega_0^2}\left[\frac{1+a^2}{(1+\phi)^2} - 1\right], \tag{6b}$$

where $\tau = \omega_0(t - z/c)$ is the time in the accompanied system of coordinates, $\tilde{z} = cz/2\omega_0 r_0^2$, $\tilde{r} = r/r_0$, and $\beta = (\omega_p r_0/c)^2$, and r_0 is the initial size of the laser beam. It is a generalization of the equations, which are conventionally used to study the processes in the case of quasimonochromatic fields, to the case of wideband radiation [19–22]. For the sake of simplicity, the tilde sign is omitted hereinafter.

With our limited computational resources, we have to limit ourselves to the one-dimensional (1D) axial plasma motion which cannot give blowout. There is no comparable way to simulate the 2D (r,z) cold electron plasma movement and guarantee avoidance of crossing singularities. A test of this using a particle code (3D PIC or circular 2D) would require enormously greater resources. Assuming these to become available, such a system could be used to test the evolution of a section of a given 1D cold run (probably using a moving-box simulation). However, for sufficiently wide initial conditions, radial motions seem *a priori* unlikely to change the basic character of results obtained here (where the radial motion is forbidden).

The system of equations (6) is much more complicated and describes a greater number of nonlinear effects than the corresponding equations for the quasimonochromatic radiation,

$$i\frac{\partial \Psi}{\partial z} + \frac{\omega_{pl}^2}{\omega_0^2}\frac{\partial^2 \Psi}{\partial \tau^2} + \Delta_\perp \Psi + \frac{\Psi\phi}{1+\phi} = 0, \tag{7a}$$

$$\frac{\partial^2 \phi}{\partial \tau^2} = \frac{1 + |\Psi|^2 - (1+\phi)^2}{2(1+\phi)^2}, \tag{7b}$$

where Ψ is the slowly changing complex amplitude of the vector potential. The second term in Eq. (7a) allows for the frequency dispersion of the background plasma. In this case, as it follows from the continuity equation for the vector potential,

$$i\frac{\partial|\Psi|^2}{\partial z} = \frac{\omega_p^2}{\omega_0^2}\frac{\partial}{\partial\tau}\left(\Psi\frac{\partial\Psi^\star}{\partial\tau} - \Psi^\star\frac{\partial\Psi}{\partial\tau}\right) + \nabla_\perp(\Psi\nabla_\perp\Psi^\star - \Psi^\star\nabla_\perp\Psi), \quad (8)$$

the total "energy" (number of quantums) of the laser pulse,

$$W_0 = 2\pi\iint|\Psi|^2 r\,dr\,d\tau, \quad (9)$$

is retained in the evolution process, i.e., the energy loss due to the excitation of plasma oscillations is not allowed for. Here and later, double integrations are performed in infinite ranges.

Note that the corresponding integral for total energy is absent within the framework of initial system (6), since W_0 decreases when the plasma wake wave is excited. When considering the processes qualitatively, we will refer repeatedly to Eqs. (7a), (7b), and (9). The matter is that the dynamics of the self-action of quasimonochromatic radiation has been studied fairly well. The effects studied within the framework of Eqs. (7a) and (7b), i.e., self-focusing instability, collapse, frequency conversion, etc., manifest themselves independently and in many cases can be quantified separately. Hereinafter, we will use these results both for setting of the most optimal initial conditions for numerical calculations, and for discussing of the obtained data.

III. ANALYSIS OF THE MODIFICATION OF THE LASER-PULSE SPECTRUM

As mentioned in the Introduction to this paper, a required condition for the shortening of a laser pulse is the widening of its spectrum under the conditions of the plasma wake-wave excitation. Therefore, at the initial stage, it is reasonable to analyze the modification of the laser-pulse spectrum in the process of nonstationary self-focusing. To illustrate specific features of the self-action dynamics for pulses with small numbers of field periods, let us turn to the numerical solution of the system of equations (6a) and (6b).

Figure 1 shows a typical intensity dynamics of the field and spectrum of the optical pulse, whose initial duration τ_p is less than the period $T_{pl} = 2\pi/\omega_{pl}$ ($\tau_p \simeq 0.09T_{pl}$) of the plasma wave. At the input to the nonlinear medium, a pulse with the following form was set:

$$a(\tau,r) = a_0\exp\left(-2\ln 2\frac{\tau^2}{\tau_p^2} - \frac{\ln 2}{2}r^2 + i\tau\right). \quad (10)$$

Since the self-action of the laser pulse is related to the excitation of the plasma wake wave, the leading edge of the pulse propagates in the unperturbed plasma (linear medium), whereas the rest of the pulse propagates in the perturbed plasma region. As it follows from Fig. 1(a), the front part of the pulse diffracts, while the self-focusing starts developing in the rear part of the pulse, and the spectrum is converted to the long-wave part [see Fig. 1(b)]. If one ignores the ruggedness of the intensity of the laser pulse $I(z,\tau,r) = |E|^2$, where

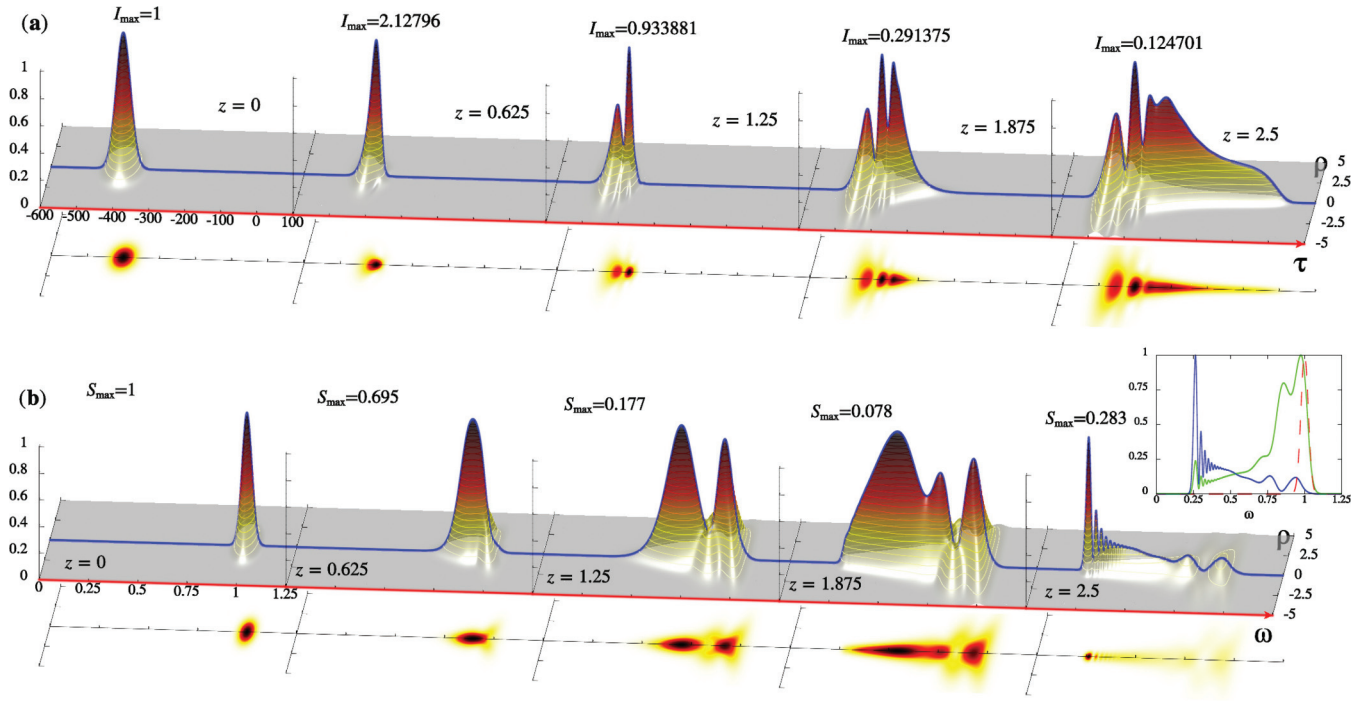

FIG. 1. (Color online) Dynamics of the circularly polarized optical field with the following initial parameters: $\tau_p = 15\pi$, $a_0 = 1.8$, and $\kappa = \tau_p\omega_{pl} = 0.555$. Here, panel (a) shows the distribution of the pulse intensity $|E|^2$ and panel (b) shows the distribution of the spectral intensity $S(\omega) = |\int E(\tau,r)e^{i\omega\tau}d\tau|^2$. The inset shows the following spectrum distributions: red dash is the initial spectrum on the beam axis, blue line is the output pulse spectrum on the beam axis, and green (light gray) line is the spectrum averaged over the output pulse beam ($|\int S(\omega,r)r\,dr|^2$).

$E(z,\tau,r) = -\partial a/\partial\tau$, then, as it follows from Fig. 1(a), the spatiotemporal distribution of the pulse acquires the form of a *horn* opening towards the leading edge of the pulse as a result of nonstationary self-focusing. It is seen from Fig. 1(b) that, during the self-action, significant conversion of the spectrum into the long-wave region takes place. Specifically, as it follows from the inset in Fig. 1(b), the maximum of the spectrum on the beam axis is shifted up to two octaves into the red region of the spectrum.

To study qualitatively the conversion of the optical pulse spectrum, we will turn to system of equations (7). During the process of nonstationary self-action at the wake wave, which is being considered, a down-spectrum frequency shift takes place. We will use the following relationship to describe this effect:

$$\langle\omega\rangle = -\frac{1}{2}\frac{d\langle\tau\rangle}{dz}. \tag{11}$$

It relates the average wave field frequency $\langle\omega\rangle$,

$$W_0\langle\omega\rangle = 2\pi\iint \omega|\Psi(\omega,r_\perp)|^2 r\,dr\,d\omega, \tag{12}$$

and the center of mass of the packet $\langle\tau\rangle$:

$$W_0\langle\tau\rangle = 2\pi\iint \tau|\Psi|^2 r\,dr\,d\tau. \tag{13}$$

The following relationship for the center of mass of the packet can be found from Eqs. (7a) and (8):

$$W_0\frac{d^2\langle\tau\rangle}{dz^2} = 4\pi\frac{\omega_{pl}^2}{\omega_0^2}\iint|\Psi|^2\frac{\partial}{\partial\tau}\left(\frac{\phi}{1+\phi}\right)r\,dr\,d\tau. \tag{14}$$

Hence it follows that during propagation of the pulse, the wave field center of mass $\langle\tau\rangle$ shifts towards the rear part of the pulse. We will estimate this effect for the case of an ultrashort pulse ($\tau_p\omega_{pl} \ll 1$) in rarefied plasma ($\omega_{pl}^2/\omega_0^2 \ll 1$) using the self-similar solutions found in [19] at $\phi \ll 1$.

In the linear focal region, when the field at the leading edge of the pulse stays almost invariable, we will use the following self-similar solutions for Ψ and ϕ:

$$\Psi = \alpha u(\zeta)\exp(\alpha\tau + i\gamma z e^{2\alpha\tau}), \quad \phi = v(\zeta)\exp(2\alpha\tau), \tag{15}$$

where $\zeta = r\,\exp(\alpha\tau)$, and α and γ are positive constants. Here, α is determined by the excess of the power over the critical power of self-focusing. These solutions describe the pulses having the shape of a *horn* opening towards the direction of the motion. The structure of the main self-similar mode is characterized by the exponential radial decrease in the vector potential and the power-law decrease ($\sim\zeta^{-2}$) in the plasma-wave potential.

Thus, for a pulse with the duration τ_p, we obtain from Eq. (14) that

$$\frac{d^2\langle\tau\rangle}{dz^2} \simeq \frac{\omega_{pl}^2}{\omega_0^2}\frac{2\sigma}{\tau_p}[\exp(2\alpha\tau_p) - 1], \tag{16}$$

where $\sigma = v(\zeta = 0) \simeq 1.5$. When finding the integral with respect to the self-similar variable ζ, we assumed that the distribution of the field in the plasma wave is smoother than the distribution of the electromagnetic field. For the shift of the center of mass $\langle\tau\rangle$, we find that

$$\langle\tau\rangle \simeq \frac{\omega_{pl}^2}{\omega_0^2}\frac{\sigma}{\tau_p}[\exp(2\alpha\tau_p) - 1]z^2. \tag{17}$$

From here, it is seen that the frequency shift $\langle\omega\rangle$ (in terms of its absolute value) increases in the linear focal region in direct proportion to z:

$$\langle\omega\rangle \simeq -\frac{\omega_{pl}^2}{\omega_0^2}\frac{\sigma}{\tau_p}[\exp(2\alpha\tau_p) - 1]z, \tag{18}$$

Out of the linear focal region ($z > z_f$), the transverse scale of the field at the leading edge of the pulse increases proportionally to z, as the pulse propagates. Therefore, to estimate the shift of the mass center of the wave packet $\langle\tau\rangle$, we will use the different self-similar solutions found in [19]:

$$|\Psi| = \alpha\frac{z_f}{z}u(\zeta)\exp(\alpha\tau), \quad \phi = \frac{z_f^2}{z^2}v(\zeta)\exp(2\alpha\tau). \tag{19}$$

Integrating Eq. (14) under the same assumptions, we find the following formula for $\langle\tau\rangle$:

$$\langle\tau\rangle \simeq \frac{\omega_{pl}^2}{\omega_0^2}\frac{2\sigma z_f^2}{\tau_p}[\exp(2\alpha\tau_p) - 1]\left[\frac{z - z_f}{z_f} - \ln\frac{z}{z_f}\right]. \tag{20}$$

For $z > z_f$, we have

$$\langle\tau\rangle \simeq \frac{\omega_{pl}^2}{\omega_0^2}\frac{2\sigma}{\tau_p}[\exp(2\alpha\tau_p) - 1]zz_f. \tag{21}$$

It is seen from expression (21) that the frequency shift $\langle\omega\rangle$ reaches its maximum at $z \gg z_f$:

$$|\langle\omega\rangle_{\max}| \simeq \frac{\omega_{pl}^2}{\omega_0^2}\frac{\sigma z_f}{\tau_p}[\exp(2\alpha\tau_p) - 1]. \tag{22}$$

Thus the shift $\langle\tau\rangle$ of the center of mass increases in compliance with the linear law in the nonlinear focal region. Hence one can obtain a more accurate estimation for the length of the pulse propagation path, along which the plasma dispersion can be neglected. Shift (21) is small compared with the pulse duration τ_p for the path

$$z \ll \frac{\omega_0^2}{\omega_{pl}^2}\frac{\tau_p^2}{2\sigma z_f}\frac{1}{\exp(2\alpha\tau_p) - 1}. \tag{23}$$

All the above relationships should be regarded as estimations, until the center of mass $\langle\tau\rangle$ shifts to a value approximately equal to the pulse duration τ_p. At long paths, the variation in the shape of the wave field starts to manifest itself. Qualitatively, it is clear that the central part of the pulse ($r \simeq 0$) shifts at a faster rate than the periphery one ($r \to +\infty$). As the center of mass $\langle\tau\rangle$ shifts towards the rear part of the pulse, self-focusing of the wave field happens in this region, where the radiation intensity is maximal. Further, one should expect that the characteristic horn-shaped structure of the pulse will be formed.

To conclude this section, we will present the results of spectrum modifications for relativistic laser pulses [Eq. (10)] under the conditions of plasma-wave excitation, which are based on solving of system of equations (6) numerically.

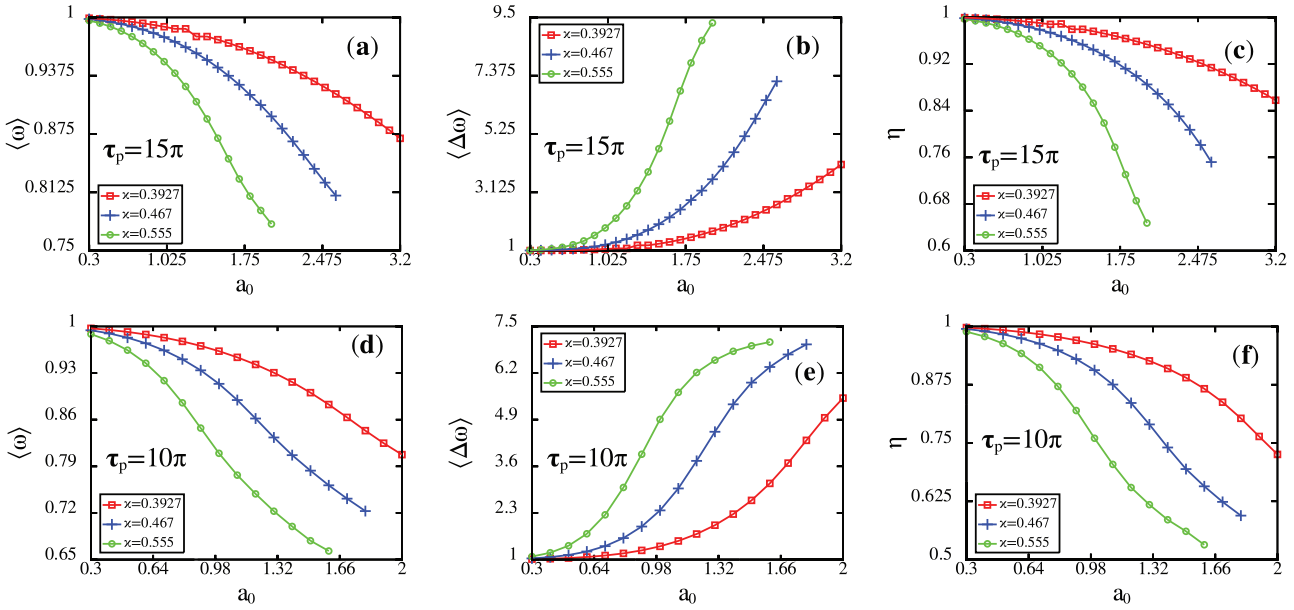

FIG. 2. (Color online) Dependences of the average carrier frequency $\langle\omega\rangle$ [(a), (d)], average spectrum width $\langle\Delta\omega\rangle = \langle\Delta\omega_{\rm out}\rangle/\langle\Delta\omega_{\rm in}\rangle$ [(b), (e)], and the relative pulse energy η [(c), (f)] depending on the initial amplitude a_0 for two different durations $\tau_p = 15\pi$, $\tau_p = 10\pi$ and plasma densities $\varkappa = \tau_p\omega_{pl}$ at the output from the nonlinear medium (at $z = 2.5$).

Figure 2 shows dependencies of the average carrier frequency,

$$P\langle\omega(z)\rangle = \iint \omega|a(z,\omega,r)|^2 d^2r_\perp d\omega,$$

$$P(z) = \iint \left|\frac{\partial a}{\partial\tau}\right|^2 d^2r_\perp d\tau,$$

and the average spectrum width

$$[P\langle\Delta\omega(z)\rangle]^2 = \iint (\omega - \langle\omega\rangle)^2|a(z,\omega,r)|^2 d^2r_\perp d\omega,$$

as well as the pulse energy $\eta(z) = P(z)/P(0)$ on the initial pulse parameters (a_0, τ_p) and on the plasma density. Since the process of the plasma wake-wave excitation is not adiabatic, it results in a decrease of the laser-pulse energy [see Figs. 2(c) and 2(f)]. It is evident that, with a decrease in the initial duration of the optical pulse, this effect becomes significant.

Let us consider the modification of the pulse spectrum separately. As seen in Fig. 2, a significant shift of the laser-pulse spectrum into the red region takes place [see also the inset in Fig. 1(b)]. For example, as it follows from the results of numerical simulation depending on the initial parameters of the problem, one can expect that the spectrum shift will be up to $\langle\omega\rangle_{\rm min} \simeq 0.65$ [see Fig. 2(d)], and the spectrum widening will reach $\langle\Delta\omega\rangle_{\rm max} \simeq 9$ [see Fig. 2(b)]. It is seen from Fig. 2 that the value of this shift depends on τ_p, since the amplitude $|a|^2_\omega$ of the spectral intensity of the vector potential, which is the source for the plasma wave [see Eq. (6b)], increases near $\omega \simeq \omega_{pl}$ as the initial duration of the laser pulse increases.

Thus, as it follows from the results of numerical simulation, a significant pulse widening takes place during the process of the self-action of the laser pulse under the conditions of the plasma wake-wave excitation. So, one can expect that under favorable conditions, it will be possible to shorten the pulse duration down to one optical cycle.

IV. SELF-COMPRESSION OF THE RELATIVISTICALLY STRONG LASER PULSE

The problems of self-compression of relativistically strong laser pulses are dealt with in several papers [15]. These papers consider the shortening of the laser pulses, whose initial duration is comparable with the period of the plasma wave. In this case, the self-compression of the laser pulse is achieved by phasing of the spectral components using the dispersion of the background plasma, since in the front part of the pulse, the frequency shifts to the red region of the spectrum, and in the rear part, to the blue region. The trailing edge of the pulse overtakes the leading edge during the pulse propagation since the group-velocity dispersion in plasma is anomalous. Evidently, this regime of laser radiation compression is also realized in the one-dimensional case. However, as mentioned in the Introduction, the main drawback of this pulse compression scheme is the rigid relationship between the initial pulse duration and the period of the plasma wave, which leads to a limitation of the energy in the initial laser pulse.

This section presents the results related to the self-compression of relativistically strong laser pulses in a wide range of parameters (plasma density and pulse energy). As shown in the previous section, the increase in the interaction length, which is achieved due to self-channeling of the pulse in the plasma in the regime of the relativistic nonlinearity saturation, leads to a significant transformation of the laser-pulse spectrum. As shown in [23], the self-focusing regime is stable under the conditions of the plasma-wave excitation, since in this case, the critical power has the initial sense of the minimal power, at which the self-focusing of the beam takes place.

Nonstationary self-action of the laser radiation evidently results in a decrease in the pulse duration. In the self-similar

regime (15), the pulse is shortened to the value equal to $\sim 1/\alpha$, i.e., the compression can be noticeable under the conditions of the significant excess of the power over the critical value. Let us dwell on this effect in more detail. To study the variations in the pulse duration qualitatively, we will use the method of momenta, as mentioned above. For the second-order momentum $\langle(\tau - \langle\tau\rangle)^2\rangle$, the following formula can be easily obtained from Eqs. (7) and (8) with an accuracy up to the first-order terms with respect to the dispersion parameter $(\omega_p^2/\omega_0^2 \ll 1)$:

$$\frac{d^2\langle(\tau - \langle\tau\rangle)^2\rangle}{dz^2} \simeq -\frac{4\pi}{W_0}\frac{\omega_{pl}^2}{\omega_0^2}\iint \frac{\phi}{1+\phi}\frac{\partial}{\partial\tau}(\tau|\Psi|^2)r\,dr\,d\tau. \tag{24}$$

Here, W_0 is the wave-packet energy [see Eq. (9)], and $\langle\tau\rangle = 2\pi W_0^{-1}\iint \tau|\Psi|^2 r\,dr\,d\tau$ is the intensity center of the wave packet. Within the self-similar solution for the field in the case of quasimonochromatic radiation [19], one can obtain the formula for the length of media

$$z_c \simeq \frac{\omega_0^2}{\omega_{pl}^2}\frac{2\tau_0^3}{\pi\alpha\mu[\exp(2\alpha\tau_0) - 1]}, \tag{25}$$

at which the pulse duration becomes zero. Here $\mu = \int_0^{+\infty}[(dv/d\zeta)^2\zeta^2 + 4v^2 + 4v(dv/d\zeta)]d\zeta$; τ_0 is the initial pulse duration. It follows from the formula for z_c that the exponential decrease in the self-compression length occurs in the self-similar regime if the power exceeds the critical value significantly $(\alpha\tau_p \gg 1)$.

To verify the obtained qualitative result, we will use numerical simulation of system (6) studying the compression of laser pulses with two different types of initial conditions. In the first calculation series, we will specify such an input triangular pulse rise, followed by an exponential decrease $\alpha = \ln 2/(8\pi^2)$, which has the shortest path of reaching the self-similar regime:

$$a = a_0\exp(-r^2\ln\sqrt{2} + i\tau) \times \begin{cases} \tau/\tau_p, & 0 \leqslant \tau < \tau_p, \\ \exp[-\alpha(\tau - \tau_p)^2], & \tau \geqslant \tau_p. \end{cases} \tag{26}$$

In the second series, the pulse has the super-Gaussian form:

$$a = a_0\exp[-r^2\ln\sqrt{2} + i\tau - 32\ln 2(\tau/\tau_p)^6]. \tag{27}$$

The results of the numerical simulation are described below. Figure 3 shows the dynamics of the field intensity for two different temporal pulse shapes, Eqs. (26) and (27). Also, there are inplots which show average spectrum width $\langle\Delta\omega\rangle$ and average frequency $\langle\omega\rangle$ of the wave field. The relative pulse energy η is shown on the bottom inplot. Note that the relative pulse energy is decreased due to wake-wave excitation at propagation in plasma.

As it follows from Fig. 3(a), the optical pulse is compressed in both the transverse and longitudinal directions, as it propagates through nonlinear medium. Additionally, as it follows from Fig. 3, the maximum compression of the pulse to two periods of the field takes place at the path $z = 0.6875$. The degree of the compression amounted to 3.6. Further, the pulse starts elongating due to the influence of the background plasma dispersion.

In the second calculation series, the initial distribution corresponding to Eq. (27) was specified. It follows from the results of the numerical simulation that, as the laser pulse propagates in a nonlinear medium, the temporal structure of the field is transformed into a structure being close to the self-similar one, and then significant compression of the laser pulse occurs [see Fig. 3(b)]. It is seen from the figure that the pulse was compressed by 11.5 times at the length $z = 1.1625$, which corresponds to a pulse with the 1.5 field period, and this duration is close to the extremely short duration of the pulse with a given spectrum width being equal to one field period. As seen from Fig. 3(b), the field intensity is amplified by 12.8 times, which is related to the field focusing in both the transverse and longitudinal directions.

The pulse with the super-Gaussian profile [Fig. 3(b)] is compressed stronger than the triangular pulse. The reason for that is that there are two stages of pulse compression. At the first stage, the pulse is compressed when the super-Gaussian profile of the pulse is transformed to the self-similar profile $(z \sim 0.4)$. At the second stage, the pulse is compressed similarly to the triangular pulse.

It follows from Fig. 4(a) that significant widening of the laser-pulse spectrum takes place during the process of the pulse self-compression. The top inset in Fig. 3(b) shows the averaged characteristics of the spectrum; from there it is seen that the pulse spectrum shifts by 25%, but widens by 11 times simultaneously. At this its energy is decreased by about 30% as it is seen from Fig. 3(b). Figure 4(b) presents the distributions of the laser-pulse intensity at the axis $(r = 0)$ at the input and output of the nonlinear medium. Along with the narrow compressed part, "wings" are present in the intensity distribution. The complete phase compensation allows one to achieve optimal *self-compression* of the output pulse, when its duration is determined only by the spectrum width. The result of the optimal *self-compression* can be obtained by the inverse Fourier transform of the spectrum shown in Fig. 4(b) (magenta dash). As follows from the figure, a pulse with a duration being equal to one field period can be obtained from the spectrum in Fig. 4(a). The compressed pulse can be categorized as an extremely short one; in this case it is slightly longer than one field period. The performed numerical experiments demonstrate sufficiently high efficiency of the proposed method, both for its energy efficiency (tens of percents), and, to a certain degree, ease of realization, where the most tender spot is the determination and right choice of the length of the nonlinear medium. It is important to note that *self-compression* of the pulse over the beam cross section is almost uniform in our numerical simulation.

As seen from Figs. 3(b) and 4(b), a compressed laser pulse has a prepulse, which is determined by the nonshifted part of the field spectrum. Therefore, if one cuts out the spectral component of the laser pulse starting at the frequency $\omega_{\text{cut}} = 0.7$ [this boundary is shown by the dashed magenta line in Fig. 4(a)], one can obtain the pulse shown in Fig. 4(b). However, by eliminating the prepulse, we increase the duration of the compressed pulse, since we cut out some of the spectral components. In this case, the pulse duration increased by 1.4 times as a result of the action of the frequency filter.

To conclude this section, the following should be emphasized. This mechanism of laser-pulse shortening is

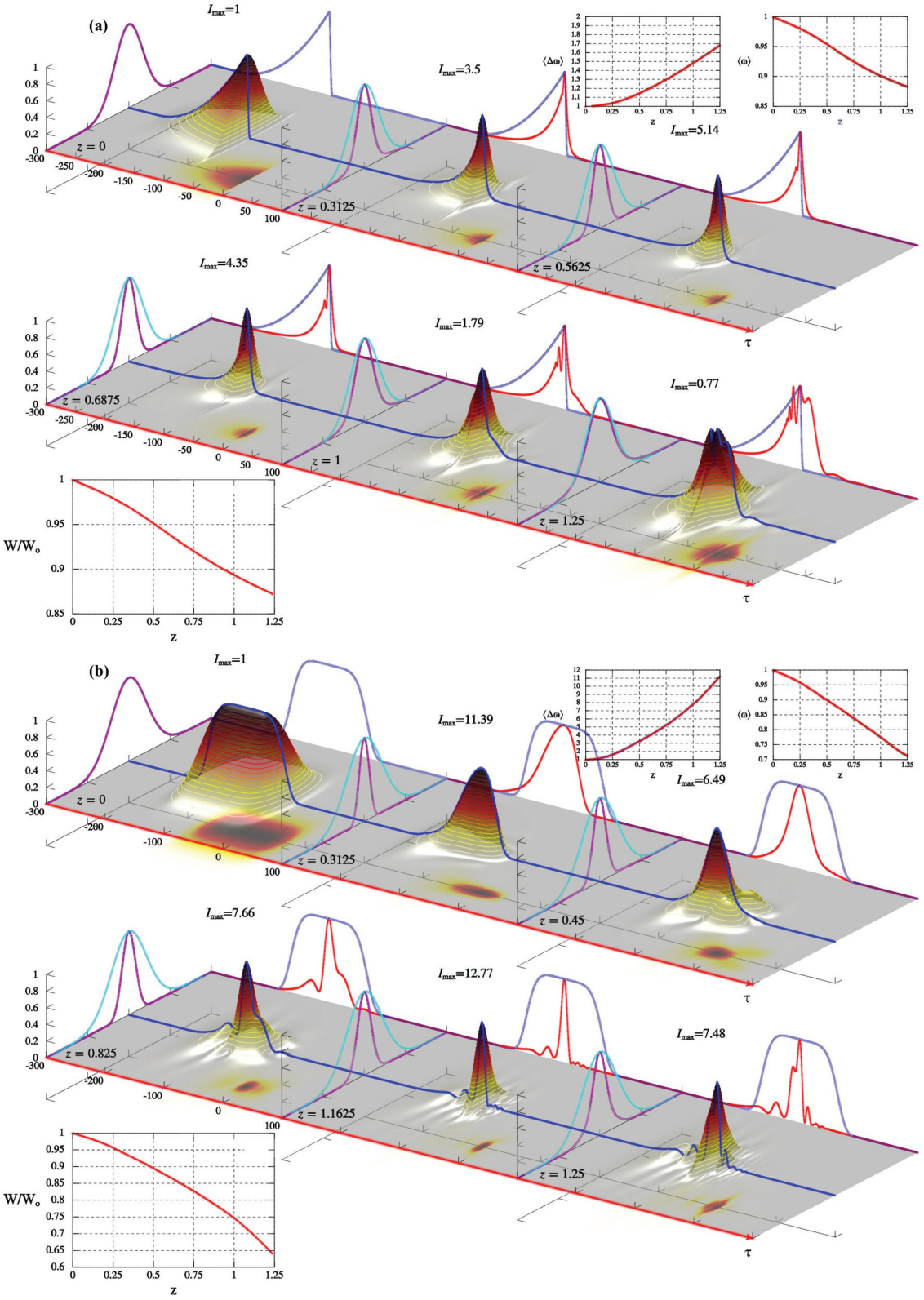

FIG. 3. (Color online) Dynamics of the intensity of the laser pulse $I(z,x,\tau) = |E(z,x,\tau)|^2$ ($E = -\partial a/\partial\tau$) for two different types of the initial conditions: (a) $\tau_p = 48\pi$, $a_0 = 2.4$, and $\tau_p = 0.07T_{pl}$; (b) $\tau_p = 40\pi$, $a_0 = 2.0$, and $\tau_p = 0.4T_{pl}$. The top left-hand panel shows the dependence of the average width of the laser-pulse spectrum $\langle\Delta\omega\rangle$; the top right-hand panel shows the average carrier frequency $\langle\omega\rangle$; the lower panel shows the relative pulse energy η. The main panel shows the laser-pulse intensities at different z values for the same coordinates. Here, the light blue (light gray) line at background shows the initial temporal profile of the laser pulse at the beam axis, the red (gray) line at background shows the current temporal profile of the pulse at the beam axis, the cyan (light gray) line shows the initial distribution of the field intensity in the transverse direction, and the magenta (gray) line shows the current distribution of the laser pulse in the transverse direction.

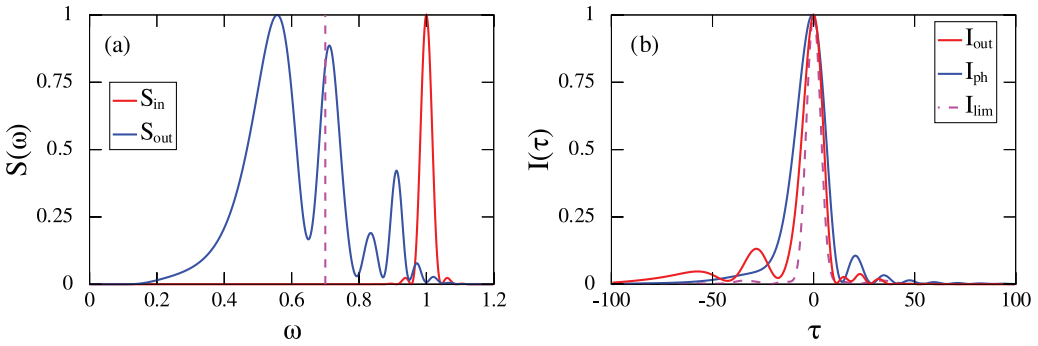

FIG. 4. (Color online) (a) Spectra of the laser pulse: red line is initial spectrum of the field, blue dots is spectrum of the compressed pulse, and magenta dash is boundary of the frequency-filter action. (b) Temporal profiles of the laser-pulse intensity: red line is compressed pulse at the length $z = 1.1625$, magenta dash is spectrum-limited pulse corresponding to the spectrum in panel (a), and blue dots is result of the action of the frequency filter on the compressed pulse (red line).

fundamentally related to the nonstationary nature of the self-focusing of the 3D wave packet during plasma wake excitation with the period longer than the initial duration of the laser pulse. Such self-compression of laser pulses takes place under the following conditions: (a) the initial beam width r_0 should exceed the plasma wavelength ($r_0 > c/\omega_p$) for a stronger self-focusing effect; (b) the initial pulse duration should be smaller than the plasma period ($\tau_p < 2\pi/\omega_p$). The main difference from other problems of laser-plasma interaction [15,16] is the use of laser beams with widths being about several hundred of microns. Obviously, it results in that the laser-pulse self-compression will take place for laser powers being about several PW or higher. In application to available laser systems [24], the numerical simulations show that the laser pulse with duration $\tau_p = 53$ fs (20 optical cycles), $a_0 = 0.7$, $\lambda = 0.8$ μm, and $r_0 = 120$ μm (that corresponds to power $P_0 = 1.1$ PW) will be compressed to a 7 fs pulse during its propagation through nonlinear media with a length of 15.8 cm and the unperturbed plasma density $n_e \simeq 7 \times 10^{17}$ cm^{-3}. Stronger compression is achieved by using higher powers. For example, a laser with a power of 10 PW will allow one to compress a pulse from a duration of 53 fs to 4 fs (1.5 optical cycles) along a path of 59 cm [see Fig. 3(b)].

Thus, to implement this laser-pulse self-compression method, one must have a plasma column several dozens of centimeters long with the transverse scale of a few hundred micrometers and electron density of 7×10^{17} cm^{-3}. Several ways to generate such plasma can be suggested as follows.

(1) The plasma can be produced by electron beam. So, a similar plasma column 65 cm long, arising as a result of the lithium vapor ionization by an electric field of the injected electron beam was used in the SLAC experiment on the wakefield acceleration of electrons [25].

(2) The plasma can be produced by the same laser pulse which is planned to be compressed. Since it concerns shortening of the laser pulse of the petawatt power level, so the intensity of a laser pulse focused for the size of 300 μm will account for 3×10^{18} W/cm^2, that far exceeds (by several orders) the ionization threshold of hydrogen 2×10^{14} W/cm^2.

(3) Besides, the plasma can be produced via the supplementary subpetawatt ionizing laser pulse advancing the main relativistic pulse by a few hundred femtoseconds to avoid the hydrodynamic plasma spread. So long as the ionizing laser pulse may become refracted one needs to set the initial intensity and the beam diameter with a considerable reserve.

It must be noted that the process of laser pulses self-compression at the self-focusing regime is weakly sensitive to the plasma inhomogeneity. Further we will consider the influence of one of the strongest instabilities (the hose instability) on the laser pulses self-compression process.

V. STABILITY OF THE REGIME OF SELF-COMPRESSION OF THE LASER PULSE

As shown in the previous section, at the optimal initial parameters of the laser radiation, one can achieve significant compression of the pulse (by more than an order of magnitude). In this case, an appropriate question arises about how various instabilities of the laser beam will influence this process of the pulse self-compression (*filamentation instability*, *hose instability* [26,27], and so on). It follows from [23,28] that the development of spatiotemporal (filamentation) instability of the laser pulse under the conditions of excitation of a plasma wave with a period exceeding the duration of the laser pulse is suppressed to a significant degree. Unlike the case of a medium with inertia-free nonlinearity, the initial stratification of the wave beam develops only at the initial stage of the process, and then filaments are attracted and the symmetric self-focusing regime is restored. In this section, we will present the results of studying the stability of the self-compression regime of a relativistically strong laser pulse with respect to the violation of the axial symmetry of the initial distribution.

Numerical analysis of this problem within the framework of the $(3+1)$-dimensional model,

$$\frac{\partial^2 a}{\partial z \partial \tau} + \frac{\beta a}{1+\phi} - \frac{\partial^2 a}{\partial x^2} - \frac{\partial^2 a}{\partial y^2} = 0, \tag{28a}$$

$$\frac{\partial^2 \phi}{\partial \tau^2} = \frac{\omega_p^2}{\omega_0^2} \frac{1 + |a|^2 - (1+\phi)^2}{2(1+\phi)^2}, \tag{28b}$$

is an extremely complicated problem due not only to insufficient computational resources, but also to the difficulty of representing the results of computer simulation of a nonstationary three-dimensional problem. Therefore, we followed the papers in [23,29,30]; specifically, while retaining the scaling of the

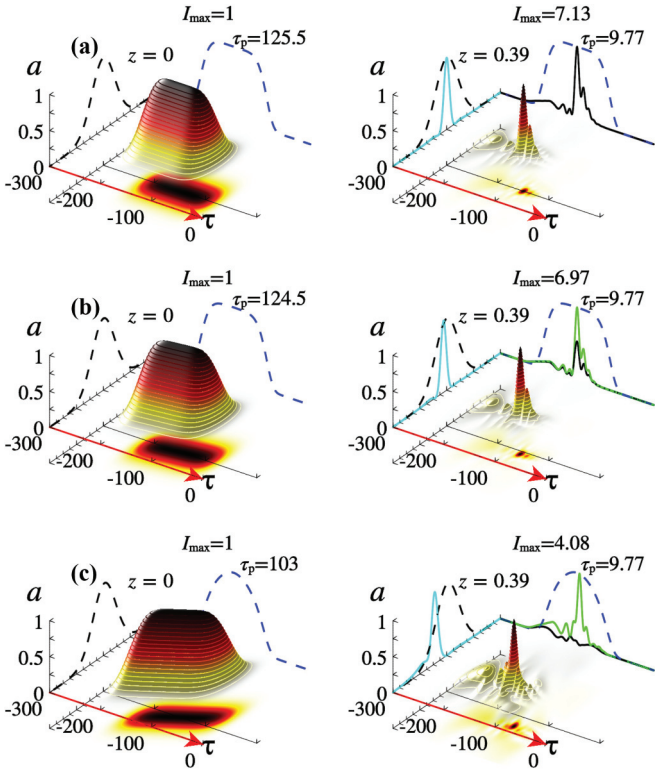

FIG. 5. (Color online) Results of the self-compression of the laser pulse specified at the input to the nonlinear medium in the form of Eq. (30) ($a_0 = 1.2$, $\kappa = 0.83$, and $\tau_p = 40\pi$) at various values of the coefficient d_1: $d_1 = 0$, $d_1 = 0.5$, and $d_1 = 2$ (a, b, and c, respectively). The left-hand panel shows the initial distribution of the field intensity; the right-hand panel shows the result of numerical simulation of the system of equations (29). Here, the dashed blue line shows the initial temporal profile of the laser pulse at the beam axis; the black line shows the current temporal profile of the pulse at the beam axis; the green (gray) line shows the temporal profile of the pulse at $x = x^*$ (in the cross section of the beam, where the intensity reaches the maximum value), the dashed black line shows the initial distribution of the field intensity in the transverse direction, and the cyan (light gray) line shows the current distribution of the laser pulse in the transverse direction.

equations, we reduced the number of spatial variables and increased the nonlinearity degree at the same time. The dynamics of the self-action of a relativistically strong laser pulse was simulated numerically by using the following system of equations:

$$\frac{\partial^2 a}{\partial z \partial \tau} + \frac{\beta a}{1+\phi} - \frac{\partial^2 a}{\partial x^2} = 0, \tag{29a}$$

$$\frac{\partial^2 \phi}{\partial \tau^2} = \frac{\omega_p^2}{\omega_0^2} \frac{1 + |a|^4 - (1+\phi)^2}{2(1+\phi)^2}. \tag{29b}$$

To study the details of the influence of structural perturbations on the process of laser-pulse shortening, we specified the initial distribution of the laser field, which was close to that considered in [31]:

$$a(x,\tau) = a_0 \exp\left(-\frac{\ln 2}{2}(x - d_1\tau/\tau_p)^2 - 32\,\ln 2(\tau/\tau_p)^6\right). \tag{30}$$

As it follows from this formula, as the coefficient d_1 increases, the main axis of the elliptical structure of the spatially confined pulse makes a turn. This corresponds to an increasingly great deviation of the laser-pulse propagation direction from the z axis. Figure 5 shows the results of the self-compression of the pulse specified at the input to the nonlinear medium in the form of Eq. (30). It is seen from the figure that the self-compression regime is stable at the considered paths of the pulse propagation. The turn of the main axis of the ellipse of the spatially confined pulse results in slight weakening of the pulse self-compression and the wing in the front part of the pulse becomes more pronounced. This arises due to the fact that, as the value of the coefficient d_1 increases, the efficient duration of the incident pulse decreases. Since we do not vary the density of the background plasma, this leads to a decrease in the efficiency of plasma-wave excitation by the incident pulse, in contrast with the case when $d_1 = 0$. Hence the quality of the phase self-modulation of the incident pulse becomes worse at a fixed length of the nonlinear medium.

VI. CONCLUSION

The paper proposes a concept for development of a plasma compressor for generation of extremely short relativistically strong femtosecond pulses at the petawatt power level. The proposed compression mechanism is basically related to the process of nonstationary self-focusing of a spatially confined wave packet in transparent plasma during excitation of a plasma wake wave with a period which exceeds the duration of the laser pulse. It is shown that, in the optimal regime, laser pulses with durations up to one optical period of the field can be excited with an energy efficiency of 25%. It is demonstrated that the regime of the laser-pulse self-compression is stable at the considered propagation paths with respect to perturbations of the axial symmetry of the initial distribution.

ACKNOWLEDGMENT

The paper was supported by the RFBR (Projects No. 11-02-00225, No. 12-02-00650, No. 12-02-33074, and No. 13-02-00755) and RF President Grant No. MK-5853.2013.2.

[1] T. Kobayashi, A. Shirakawa, and T. Fuji, IEEE J. Sel. Top. Quantum Electron. **7**, 525 (2001).
[2] G. A. Mourou, T. Tajima, and S. V. Bulanov, Rev. Mod. Phys. **78**, 309 (2006).
[3] V. B. Gildenburg and N. V. Vvedenskii, Phys. Rev. Lett. **98**, 245002 (2007).
[4] A. V. Kim, M. Yu. Ryabikin, and A. M. Sergeev, Phys. Usp. **42**, 54 (1999).
[5] A. Baltuska *et al.*, Nature (London) **421**, 611 (2003).
[6] M. Nisoli, S. De Silvestri, and O. Svelto, Appl. Phys. Lett. **68**, 2793 (1996).
[7] G. Tempea and T. Brabec, Opt. Lett. **23**, 1286 (1998).

[8] A. A. Babin, D. V. Kartashov, A. M. Kiselev, V. V. Lozhkarev, A. M. Sergeev, A. A. Solodov, and A. N. Stepanov, Pis'ma Zh. Eksp. Teor. Fiz. **76**, 645 (2002) [JETP Lett. **76**, 548 (2002)].

[9] C. P. Hauri *et al*., Appl. Phys. B **79**, 673 (2004).

[10] N. L. Wagner, E. A. Gibson, T. Popmintchev, I. P. Christov, M. M. Murnane, and H. C. Kapteyn, Phys. Rev. Lett. **93**, 173902 (2004).

[11] S. A. Skobelev, D. I. Kulagin, A. N. Stepanov, A. V. Kim, A. M. Sergeev, and N. E. Andreev, Pis'ma Zh. Eksp. Teor. Fiz. **89**, 641 (2009) [JETP Lett. **89**, 540 (2009)].

[12] G. Stibenz, N. Zhavoronkov, and G. Steinmeyer, Opt. Lett. **31**, 274 (2006).

[13] S. Skupin, G. Stibenz, L. Berge, F. Lederer, T. Sokollik, M. Schnurer, N. Zhavoronkov, and G. Steinmeyer, Phys. Rev. E **74**, 056604 (2006).

[14] O. G. Kosareva, I. N. Murtazin, N. A. Panov *et al*., Laser Phys. Lett. **4**, 126 (2007).

[15] J. Faure, Y. Glinec, J. J. Santos, F. Ewald, J. P. Rousseau, S. Kiselev, A. Pukhov, T. Hosokai, and V. Malka, Phys. Rev. Lett. **95**, 205003 (2005); O. Shorokhov, A. Pukhov, and I. Kostyukov, *ibid*. **91**, 265002 (2003); M. Lontano and I. G. Murusidze, Opt. Express **11**, 248 (2003).

[16] E. Esarey, C. B. Schroeder, and W. P. Leemans, Rev. Mod. Phys. **81**, 1229 (2009).

[17] A. A. Balakin, A. G. Litvak, V. A. Mironov, and S. A. Skobelev, Zh. Eksp. Teor. Fiz. **131**, 408 (2007) [JETP **104**, 363 (2007)]; Phys. Rev. A **80**, 063807 (2009).

[18] D. V. Kartashov, A. V. Kim, and S. A. Skobelev, Pis'ma Zh. Eksp. Teor. Fiz. **78**, 722 (2003) [JETP Lett. **78**, 276 (2003)]; S. A. Skobelev, D. V. Kartashov, and A. V. Kim, Phys. Rev. Lett. **99**, 203902 (2007); A. V. Kim, S. A. Skobelev, D. Anderson, T. Hansson, and M. Lisak, Phys. Rev. A **77**, 043823 (2008).

[19] L. A. Abramyan, A. G. Litvak, V. A. Mironov, and A. M. Sergeev, Zh. Eksp. Teor. Fiz. **102**, 1816 (1992) [JETP **75**, 978 (1992)].

[20] S. V. Bulanov, F. Pegoraro, and A. M. Pukhov, Phys. Rev. Lett. **74**, 710 (1995); N. E. Andreev, V. I. Kirsanov, A. A. Pogosova, and L. M. Gorbunov, Pis'ma Zh. Eksp. Teor. Fiz. **60**, 694 (1994) [JETP Lett. **60**, 713 (1994)].

[21] P. Sprangle, E. Esarey, J. Krall, and G. Joyce, Phys. Rev. Lett. **69**, 2200 (1992).

[22] S. V. Bulanov and A. S. Sakharov, Pis'ma Zh. Eksp. Teor. Fiz. **54**, 208 (1991) [JETP Lett. **54**, 203 (1991)].

[23] A. A. Balakin, A. G. Litvak, V. A. Mironov, and S. A. Skobelev, Zh. Eksp. Teor. Fiz. **139**, 579 (2011) [JETP **112**, 504 (2011)].

[24] J. H. Sung, S. K. Lee, T. J. Yu, T. M. Jeong, and J. Lee, Opt. Lett. **35**, 3021 (2010); X. Liang, Y. Leng, C. Wang, C. Li *et al*., Opt. Express **15**, 15335 (2007).

[25] I. Blumenfeld, C. E. Clayton, F.-J. Decke, M. J. Hogan *et al*., Nature (London) **445**, 741 (2007).

[26] P. Sprangle, J. Krall, and E. Esarey, Phys. Rev. Lett. **73**, 3544 (1994).

[27] G. Shvets and J. S. Wurtele, Phys. Rev. Lett. **73**, 3540 (1994).

[28] N. E. Andreev, L. M. Gorbunov, P. Mora, and R. Ramazashvili, Phys. Plasmas **14**, 083104 (2007).

[29] A. G. Litvak, A. M. Sergeev, and V. A. Mironov, in *Nonlinear Waves 3*, edited by A. V. Gaponov-Grekhov, M. I. Rabinovich, and J. Enqelbrecht (Springer-Verlag, Berlin-Heidelberg, 1990), p. 240.

[30] A. G. Litvak, A. M. Sergev, and V. A. Mironov, Phys. Scr. **30**, 57 (1990).

[31] M. C. Kaluza, S. P. D. Mangles, A. G. R. Thomas, Z. Najmudin, A. E. Dangor, C. D. Murphy *et al*., Phys. Rev. Lett. **105**, 095003 (2010).